Imaging Magnetic Domains with Sub-Micrometer Resolution

C.M. SCHNEIDER[1,2], R. FRÖMTER[2], C. ZIETHEN[1], G. SCHÖNHENSE[1], J. KIRSCHNER[2]

[1)]*Inst. f. Physik, Joh. Gutenberg-Universität, Staudingerweg 7, D-55099 Mainz, Germany*
[2)]*Max-Planck-Institut f. Mikrostrukturphysik, Am Weinberg 2, D-06120 Halle (Saale), Germany*

Understanding the physical properties of magnetic microstructures is of great technological importance. A controlled and reproducible creation of well-defined magnetic domains crucially determines operation and performance of magnetic mass storage systems, e.g., a hard disk. The ongoing request for higher storage capacities in still smaller devices can only be met by increasing the storage density and therefore reducing the lateral dimensions of the individual magnetic domains which carry the information. Currently, bit sizes are of the order of some 100 nm. In order to characterize these magnetic domains, appropriate imaging techniques with a lateral resolution in the range of the domain boundaries, i.e., several 10 nm are needed. Thus not only the production, but also the characterization of these magnetic microstructures poses a considerable challenge. Conventional optical domain imaging techniques, such as magneto-optical Kerr microscopy (1), are diffraction-limited and can no longer supply the desired information.

Photoelectron Emission Microscopy

A promising approach which has the potential of pushing the lateral resolution into the 10nm range is photoelectron emission microscopy (2, 3). A photoelectron emission microscope (PEEM) employs as a principle an immersion lens objective in combination with a contrast aperture to form an image with the electrons photoemitted from the surface. This electron image is subsequently magnified by a set of projective lenses onto an image converter (multichannelplate and scintillator), where it can be visually observed and/or recorded by a camera system. When operated with synchrotron radiation from a dedicated 3rd generation facility, a PEEM strongly gains in versatility (4). First, the high brightness significantly cuts down the acquisition times and permits even real-time studies. Second, the tunability of synchrotron radiation can be exploited to introduce element selectivity into the imaging process simply by exciting characteristic electronic levels in the solid. Third, the defined polarization of synchrotron radiation forms the basis for a magnetic contrast mechanism. In particular with circularly polarized light in the soft X-ray regime the effect of magnetic circular dichroism can be conveniently employed to image magnetic domains (5, 6). Since in magnetic circular dichroism the signal (photoelectron yield) depends on the projection of the magnetization vector M onto the photon spin, or equivalently, the direction of light incidence q, magnetic domains with a local magnetization vector parallel or antiparallel to the photon spin will show up as dark and bright areas in the image. Areas with a local magnetization perpendicular to the incoming light beam, however, will show no contrast, i.e., the same level of intensity. The magnetic dichroism in the soft X-ray regime is due to the absorption process at characteristic edges (7, 8).

The electrons contributing most to the total photoelectron yield image are low energy secondary electrons created within the inelastic scattering cascade. In metallic systems the information depth of these electrons is around 20-30Å. Operated in the yield mode, i.e., without additional energy filtering of the electrons in the imaging process, a PEEM can therefore not only image surfaces, but to some extent even buried layers. This is particularly interesting in the field

of magnetic multilayers when it comes to the investigation of magnetic coupling phenomena. In the case of magnetic interlayer coupling, two ferromagnetic layers interact through a nonmagnetic spacer layer and one may be interested in the resultant magnetic microstructure in each of the magnetic layers (9). Thus, summarizing the above arguments, photoemission microscopy using soft X-rays can be regarded as a versatile imaging technique on the mesoscopic scale which offers a unique combination of magnetic sensitivity, elemental specificity, and surface selectivity.

Our experiments employed a newly developed instrument (Focus IS-PEEM). One of the important features of this device is a sample stage integrated into the electron optical column, which allows an easy positioning of the sample in front of the objective lens and improves the stability of the set-up against vibrations. The lateral resolution achieved with this instrument is better than 50 nm. The experiment is further equipped with standard surface analytical facilities for characterizing crystalline structure and chemical composition. Samples can be transferred into the vacuum by a load-lock system. The experiments were performed with circularly polarized soft X-rays taken from the PM-3 plane grating monochromator beamline at BESSY (Berlin) and at the helical undulator beamline BL26 of the ESRF (Grenoble).

Figure 1. Magnetic domain patterns in a microstructured Permalloy film grown on a Silicon wafer. The image has been recorded using magnetic circular dichroism at the Fe L3 absorption edge. The Permalloy squares have a period of 25μm. The gridlike structure corresponds to the uncovered Si surface (sample courtesy of A. Wadas and R. Wiesendanger, University of Hamburg).

Microstructured samples

In order to characterize the performance of the microscope, we investigated several microstructured samples. The first one was a 30 nm thick permalloy film ($Fe_{19}Ni_{81}$) which had been deposited through a mesh onto a silicon wafer and covered by a protective layer of gold. This procedure resulted in a regular array of squares with a period of 25 μm (Figure 1). Before inserting the sample into the microscope the gold was removed by gentle sputtering. An individual image obtained by exciting with circularly polarized light, for instance at the Fe $L_{2,3}$ edges, contains not only magnetic information, but also chemical and topography contrast. In order to separate the magnetic contrast, one may use the fact that the MCD signal reverses sign when going from the L_3 to the L_2 edge, or that it reverses sign upon a change of the light helicity. In both cases, chemical and topographic contrast mechanisms remain unaffected. A subtraction of two images acquired with opposite light helicities or at the L_3/L_2 edges eliminates the influence of nonmagnetic contrast, and a normalization to their sum quantifies the magnetic contrast and serves as a bright field correction. In the case of the permalloy microstructure such a L_3/L_2 subtraction procedure at the Fe absorption lines reveals a very regular domain pattern (Figure 1). Most of the squares in the image show an arrangement of four triangular domains, two of which are magnetized parallel and antiparallel, respectively, to the incoming light beam. The other two domains are oriented perpendicular to this direction. In all cases, however, the magnetization vector lies within the surface plane. A reconstruction of the spatial orientation of $\underline{M}$ in one of the squares is indicated by the arrows, and exhibits a typical flux closure structure. This domain structure can be understood by the fact that Permalloy is a magnetically very soft material, i.e., with small intrinsic magnetic anisotropy. As a consequence, the behavior of the magnetization in the present case is dominated

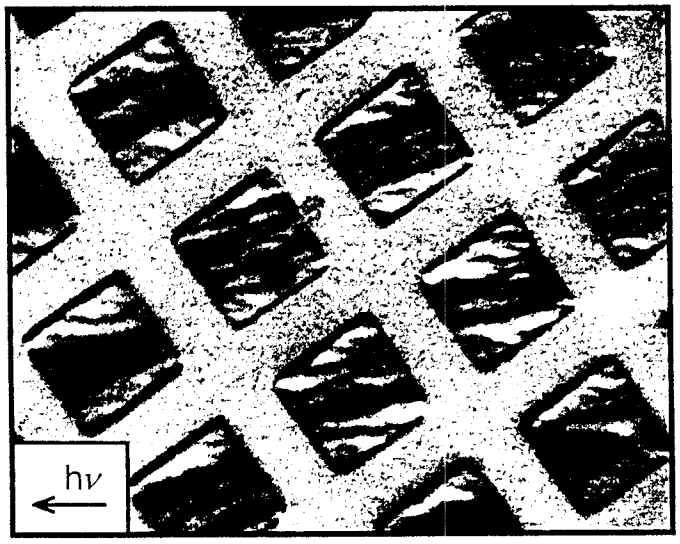

Figure 2. Magnetic microstructure in a patterned CoPt multilayer grown on a Si wafer. The image has been recorded using MCD at the Co L_3 edge. Each square has a lateral size of 20 μm × 20 μm and consists of a 50nm thick CoPt multilayer (sample courtesy of M. Huth, University of Mainz).

by the tendency of the system to minimize the magnetic stray field. For the given square shape, this is achieved by the structure observed in the experiment. This ideal case may be easily destroyed by defects, as can be seen in the square in the center of the image. It shows a more complicated domain pattern, which is pinned to a structural defect on the substrate. It should be noted that the same information about the magnetic microstructure is obtained when exciting with photon energies corresponding to the Ni $L_{2,3}$ edge.

A completely different domain pattern is observed in Figure 2. The sample was a CoPt multilayer grown on a silicon substrate. The completed multilayer was patterned by ion etching into squares of ca. 20 μm side length each. Co is known to have a very strong intrinsic magnetic anistropy which is due to spin-orbit coupling (magnetocrystalline anisotropy). The filigran feather-like domain pattern within each square therefore reflects the strong influence of the intrinsic anisotropy rather than the shape of the sample. A further difference to the Permalloy sample concerns the number of gray levels which reflect the possible spatial directions of M. A statistical analysis of the abundance of the various gray levels in the CoPt squares exhibits an almost continuous distribution, whereas one finds three distinct maxima for the Permalloy squares. This suggests that the magnetization vector in the CoPt system has a higher number of possible spatial orientations. This is compatible with the film being polycrystalline. In this case the easy axes of magnetization—as determined by the magnetocrystalline anisotropy—change with the spatial orientation of the crystallite more or less randomly. The result is a rather complex variation of M along the sample surface which is sometimes called a magnetization "ripple" (10).

Magnetic domain walls

The transition region between two neighboring domains, the so-called domain wall, represents a magnetic microstructure on a yet smaller lateral scale. The task of mapping these domain walls is thus another crucial test for the capabilities of a potential domain imaging techniques. The orientational dependence of MCD can be exploited to selectively image the magnetization component within the wall along the direction of light incidence. An example is given in Figure 3, which shows a small section from an Fe(001) single crystal surface. Because of the fourfold crystalline symmetry of the surface there are four possible orientations of M which are tied to the in-plane [100] axes. We have chosen a region of the sample where the magnetization in the domains points perpendicular to the incoming light beam. Consequently the domains themselves do not show a magnetic contrast. Their boundaries, however, show up as narrow bright and dark lines.

In order to understand this behavior we must consider the difference of domain walls in the bulk and at the surface. The domains in Figure 3 are oppositely magnetized and are thus separated by a so-called 180°-wall in which the magnetization vector rotates continuously by 180° from one orientation to the other. In the bulk the axis of rotation is normal to the wall. This case is called a Bloch wall. Note that the magnetization in the center of the Bloch wall stands perpendicular to the surface plane. Therefore, a rotation of M at the surface in a Bloch-like fashion would generate a significant magnetization component normal to the surface. An energetically more favorable situation is achieved if the magnetization vector rotates within the surface, i.e., the rotational axis lies within the wall plane and normal to the surface. This behavior is

said to be Néel-like. As a consequence, the Bloch wall in the bulk takes a Néel-like termination at the surface. It should be pointed out that the rotations of M in the Bloch- and Néel-like part of the wall are not uniquely connected. In the experiment, we therefore may observe a change of contrast along the wall at the surface. This change of rotational sense of M is limited to the near-surface region and forms a surface magnetic singularity (indicated by the circles) (11, 12).

The domain wall width at the Fe(001) surface as determined by means of scanning electron microscopy with spin polarization analysis was found to be of the order of 200 nm (11). Our measurements yield a value of ~300 nm. In fact, the magnetic resolution is currently limited by the large energy spread of the imaged electrons and the chromatic aberration of the electron-optical column. A significant improvement down to less than 50 nm can be expected if an imaging energy filter is introduced into the system.

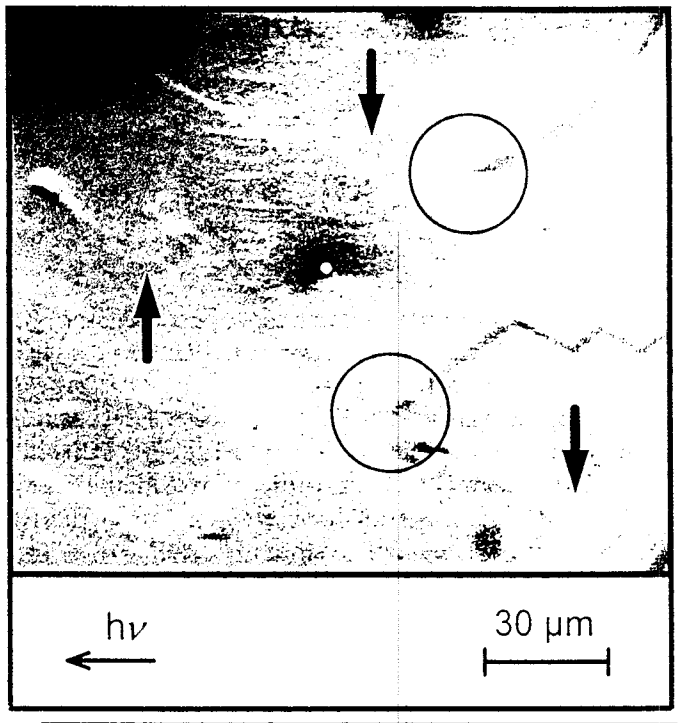

Figure 3. Magnetic domain walls at a Fe(001) surface. Only the domains in the upper part of the image (dark areas) have their magnetization vector along the direction of light incidence. All other domains are magnetized perpendicular to this direction and thus give no contrast. Their boundaries, however, show up as dark and bright zig-zag lines, because a component of the magnetization vector within the domain wall points along the incident light. The circles mark the position of surface magnetic singularities, where the rotation of the magnetization in the domain wall reverses its direction, i.e., the wall contrast changes from dark to bright and vice versa.

Outlook

The examples discussed above characterize the present status of photoemission microscopy with synchrotron radiation. Further improvements of the electron-optical set-up, e.g., the introduction of an imaging energy filter, and the increased availability of dedicated undulator beamlines for microscopy purposes, will make this method a standard technique in the mesoscopic regime. Its particular virtue lies in the combination of chemical and magnetic information. Exploiting the high photon flux delivered from undulator beamlines, future experiments on magnetic systems may even be carried out in real-time, thus studying, for example, magnetic relaxation phenomena. ■

Acknowledgments

We thank N. Brookes (ESRF) and F. Schäfers (BESSY) for their generous support during the beamtimes. The collaboration with W. Swiech from the University of Illinois in Urbana is gratefully acknowledged. The Permalloy sample was supplied by A. Wadas and R. Wiesendanger from the Institute of Applied Physics at the University of Hamburg. This work was financially supported by the Bundesminister für Bildung und Forschung under grant No. 05 644 EFA 5.

1. E. Fuchs, *Naturwiss.* **47**, 392 (1960).
2. E. Bauer and W. Telieps, in: *Surface and Interface Characterization by Electron Optical Methods*, eds. A. Howie and U. Valdrè. (Plenum Press, New York, 1988) p. 195 .
3. E. Bauer, T. Franz, C. Koziol, G. Lilienkamp, and T. Schmidt, in: *Recent Advances in LEEM/PEEM for Structural and Chemical Analyses*, ed. R. Rosei. (Kluwer Academic Publishing, Dordrecht, 1996).
4. W. Swiech, G.H. Fecher, C. Ziethen. O. Schmidt, G. Schönhense, K. Grzelakowski, C.M. Schneider, R. Frömter, and J. Kirschner, *J. Electron Spectr. and Rel. Phen.* (accepted) (1996).
5. J. Stöhr, Y. Wu, M.G. Samant, B.D. Hermsmeier, G. Harp, S. Koranda, D. Dunham, and B.P. Tonner, *Science* **259**, 658 (1993).
6. C.M. Schneider, K. Holldack, M. Kinzler, M. Grunze, H.P. Oepen, F. Schäfers, H. Petersen, K. Meinel, and J. Kirschner, *Appl. Phys. Lett.* **63**, 2432 (1993).
7. G. Schütz, W. Wagner, W. Wilhelm, P. Kienle, R. Zeller, R. Frahm, and G. Materlik, *Phys. Rev. Lett.* **58**, 737 (1987).
8. C.T. Chen, F. Sette, Y. Ma, and S. Modesti, *Phys. Rev. B* **42**, 7262 (1990).
9. J. Unguris, R.J. Celotta, and D.T. Pierce, *Phys. Rev. Lett.* **67**, 140 (1991).
10. D.J. Craik and R.S. Tebble, *Ferromagnetism and Ferromagnetic Domains*, ed. E.P. Wohlfarth, Vol. 4. (North-Holland, Amsterdam, 1965).
11. H.P. Oepen and J. Kirschner, *Phys. Rev. Lett.* **62**, 819 (1989).
12. M.R. Scheinfein, J. Unguris, J.L. Blue, K.J. Coakley, D.T. Pierce, R.J. Celotta, and P.J. Ryan, *Phys. Rev. B* **43**, 3395 (1991).